Human Molecular Genetics, 2009, Vol. 18, No. 23 ***4603–4614***
doi:10.1093/hmg/ddp427
Advance Access published on September 10, 2009

Missense mutations in the SH3TC2 protein causing Charcot-Marie-Tooth disease type 4C affect its localization in the plasma membrane and endocytic pathway

Vincenzo Lupo[1,2], Máximo I. Galindo[1,2], Dolores Martínez-Rubio[1,2], Teresa Sevilla[3,4], Juan J. Vílchez[3,4], Francesc Palau[1,2,*] and Carmen Espinós[2]

[1]Genetics and Molecular Medicine Unit, Instituto de Biomedicina de Valencia (IBV), CSIC, Valencia 46010, Spain, [2]CIBER de Enfermedades Raras (CIBERER), Valencia 46010, Spain, [3]Neurology Service, Hospital Universitari La Fe, Valencia 46009, Spain and [4]CIBER de Enfermedades Neurodegenerativas (CIBERNED), Valencia 46009, Spain

Received July 8, 2009; Revised and Accepted September 3, 2009

Mutations in *SH3TC2* (*KIAA1985*) cause Charcot-Marie-Tooth disease (CMT) type 4C, a demyelinating inherited neuropathy characterized by early-onset and scoliosis. Here we demonstrate that the SH3TC2 protein is present in several components of the endocytic pathway including early endosomes, late endosomes and clathrin-coated vesicles close to the *trans*-Golgi network and in the plasma membrane. Myristoylation of SH3TC2 in glycine 2 is necessary but not sufficient for the proper location of the protein in the cell membranes. In addition to myristoylation, correct anchoring also needs the presence of SH3 and TPR domains. Mutations that cause a stop codon and produce premature truncations that remove most of the TPR domains are expressed as the wild-type protein. In contrast, missense mutations in or around the region of the first-TPR domain are absent from early endosomes, reduced in plasma membrane and late endosomes and are variably present in clathrin-coated vesicles. Our findings suggest that the endocytic and membrane trafficking pathway is involved in the pathogenesis of CMT4C disease. We postulate that missense mutations of *SH3TC2* could impair communication between the Schwann cell and the axon causing an abnormal myelin formation.

INTRODUCTION

Charcot-Marie-Tooth (CMT) disease is the most common inherited neuropathy with a prevalence of 28 in 100 000 (1,2). CMT refers to a clinically heterogeneous group of hereditary motor and sensory neuropathies that have as main clinical features progressive distal muscle weakness and atrophy, foot deformities and distal sensory loss. CMT is separated into two groups: CMT1 or demyelinating forms with slow nerve conduction velocities (NCVs < 38 m/s) and segmental demyelination and remyelination on nerve biopsies; and CMT2 or axonal forms with normal or nearly normal NCV and nerve pathology with signs of axonal degeneration. CMT also presents a wide genetic heterogeneity, not only because 26 genes and more than 30 loci have been described to be associated with it, but also because the disease may segregate with different Mendelian patterns. Most patients present autosomal dominant CMT, although some patients develop autosomal recessive forms, which are particularly severe and disabling from infancy, named CMT4 for demyelinating forms and ARCMT2 for axonal variants. CMT4C is an early-onset demyelinating form characterized by a severe scoliosis and is due to mutations in the *SH3TC2* gene, also named *KIAA1985* (3,4).

To date, a total of 19 *SH3TC2* mutations have been identified in Caucasian non-Gypsy families from Turkey, Germany, Italy, Greece, Iran and UK (3–6). We have described two *SH3TC2* mutations, p.R1109X and p.C737_P738delinsX, in a series of

*To whom correspondence should be addressed at: Genetics and Molecular Medicine Unit, Instituto de Biomedicina de Valencia (IBV), CSIC, c/Jaume Roig, 11, Valencia 46010, Spain. Tel: +34 963393773; Fax: +34 963690800; Email: fpalau@ibv.csic.es

Spanish Gypsy families with a childhood-onset demyelinating CMT phenotype with autosomal recessive inheritance (7), postulating a founder effect for the *SH3TC2* p.R1109X in Gypsy population (7,8). Moreover, the p.R954X has been described as a founder event in the French-Canadian population (5). As a result of the characterization of these mutations affecting a number of patients, SH3TC2 has gained interest in the field of CMT research. Very little is known about SH3TC2, apart from the fact that it is a conserved protein in vertebrates, with strong expression in brain, spinal cord and sciatic nerve, and somewhat weaker expression in skeletal muscles (3). According to the presence of SH3 and TPR domains, the SH3TC2 protein probably interacts with other proteins and may be a constituent of multiprotein complexes (3).

The molecular mechanisms leading to CMT are as diverse and complex as its genetics, and the CMT-related genes code for proteins with a wide variety of roles in nervous system cells. Alterations in many of them cause demyelinating neuropathies, although in some disorders the primary lesion occurs in the axon. Moreover, muscular weakness and atrophy in demyelinating forms is secondary to axonal impairment. CMT1A, the most frequent type of CMT (9), is due to a duplication of 1.4 Mb that encompasses the *PMP22* gene (10). The PMP22 protein is a structural constituent of myelin and its overexpression leads to the formation of aggregates that alter the degradative pathway (11). MPZ/P0, related to CMT1B, and connexin32 (Cx32), causative of CMTX1, are also components of the myelin (12,13). *PMP22* and *Cx32/GJB1* are regulated by SOX10 in synergy with EGR2 (14–17) whose mutation leads to both CMT1D and CMT4E. Mitochondrial dynamics can be also impaired in CMT disease: MFN2 associated with CMT2A2, a dynamin-like GTPase involved in mitochondrial fusion, tethers endoplasmic reticulum membranes to mitochondria (18) and GDAP1, responsible for CMT4A and its allelic variants ARCMT2K and CMT2K, is required for mitochondrial fission (19–21). Other CMT proteins are involved in the regulation of protein synthesis, sorting and/or degradation. LITAF/SIMPLE, causative of CMT1C, is a small integral protein of the lysosome/late endosome that plays a role in endosomal protein trafficking and degradation (22–24). MTMR2 and MTMR13/SBF2 responsible for CMT4B1 and CMT4B2, respectively, are both phospholipid phosphatase proteins found in the cytosol. MTMR2 could be implicated in intracellular trafficking through its phosphatase activity and is regulated by heterodimerization with inactive partners, such as MTMR13/SBF2 (25,26). Rab7, mutated in CMT2B (27), and DNM2, responsible for dominant intermediate (DI) CMTB (28), take part in a wide variety of cellular mechanisms, including membrane trafficking: Rab7 is a Ras-related GTP-binding protein involved in transport from early-to-late endosomes (29–31), and DNM2 is a fission protein that participates in endocytic vesicle formation and plays a role in membrane trafficking from the late endosome and Golgi (32–35). The knowledge of the many functions to which CMT proteins contribute, and therefore the elucidation of the disease process, is far from complete. One of the most common themes to many of the proteins, and the cellular events in which they participate, is the sorting and degradation of proteins and vesicles through the endocytic pathway.

In our clinical series, CMT4C is the most frequent form of inherited peripheral neuropathy in the Gypsy population (7). Here we show results of the mutation analysis of *SH3TC2* gene in non-Gypsy families from such a series. As a first step towards understanding the pathogenic mechanisms of mutations, we have investigated the sub-cellular localization of SH3TC2 and its possible involvement with known cellular pathways. We have observed that SH3TC2 participates in the endocytic pathway of cell traffic and is also anchored to plasma membrane. We demonstrate that whereas null mutations do not affect proper localization of the truncated protein, missense mutations affect the correct localization of the protein in endosomes and plasma membrane.

RESULTS

Mutation screening of the *SH3TC2* gene

Fourteen probands were screened for mutations in the *SH3TC2* gene (see Materials and Methods). We found mutations in five of them, and two of these mutations were novel (Table 1 and Supplementary Material, Fig. S1). The first one, c.3305delA (proband ID no. 735), was homozygous. It causes a frameshift and a premature stop 14 codons downstream. The second one was found in proband ID no. 744, c.1906_1923delTGCTT TCTGGCCATCCGCinsAGGGCC, and was a compound heterozygous with the c.2860C>T change. This latter change is very interesting because it has been described to be a founder mutation in the French-Canadian population (5). We searched for both novel mutations in 200 chromosomes from healthy controls of Spanish ancestry and found neither, suggesting that they could be pathogenic. Among the rest of the already described mutations, proband ID no. 680, with an intermediate phenotype, carried the c.1586G>A change, which results in a missense p.R529Q mutation. In our series, we found two probands with the p.R1109X mutation, which is a founder mutation in Gypsies (7,8). These probands were unaware of any Gypsy ancestry, but after finding this mutation we took a more detailed history of the patients, which did reveal a Gypsy background in one patient. The other patient's origin could not be confirmed. Both probands belong to consanguineous families and we confirmed co-segregation of the DNA changes with phenotype in these two families.

Including our two novel mutations, the list of changes in *SH3TC2* has grown to more than 20, including nonsense, missense and indels mutations. Little is known about the cellular and molecular role of the SH3TC2 protein, so we decided to embark in a functional study of this protein in a cell culture system.

Cloning and cell expression of the SH3TC2 cDNA

The longest transcript described for *SH3TC2* codes for a 1288 amino acids protein (3). We obtained a cDNA with the same coding capacity by combining three partial cDNAs. The electronic annotation of the protein (SwissProt Q8TF17) reveals the presence of two SH3 and eight TPR domains. These two types of domain are involved in protein–protein interactions. In addition, we conducted an *in silico* analysis of the SH3TC2 sequence using the PSORT II software, which

Table 1. Identified mutations in the *SH3TC2* gene

Proband's family	Proband ID no.	Case type	Mutation Nucleotide change	Amino acid change	State	References
CMT-267	735	Sporadic	c.3305delA	p.H1102LfsX14	Homozygous	Novel
CMT-88	141	Familial	c.3325C>T	p.R1109X	Homozygous	(7,8)
CMT-26	609	Familial	c.3325C>T	p.R1109X	Homozygous	(7,8)
CMT-241	680	Sporadic	c.1586G>A	p.R529Q	Homozygous	(3)
CMT-210	744	Sporadic	c.1906_1923delTGCTTTCTGGCCATCCGCinsAGGGCC	p.C636_R641delinsRA	Compound	Novel
			c.2860C>T	p.R954X	heterozygous	(3)

predicted the presence of an N-myristoylation motif (MGGCFCI). N-myristoylation is a lipid anchor modification of proteins targeting them to membrane locations (36,37).

To investigate the expression and sub-cellular localization of SH3TC2, we generated two-tagged versions, one with the myc tag at the N terminus (myc-SH3TC2) and one with the HA tag at the C terminus (SH3TC2-HA). We transiently transfected the corresponding plasmids into COS-7 cells and after 24 h, we analyzed the cellular localization by immunodetection with anti-myc and anti-HA antibodies using confocal microscopy. Surprisingly, the two-tagged proteins showed a completely different sub-cellular localization. myc-SH3TC2 showed a cytoplasmic pattern that was found to co-localize with endoplasmic reticulum (Fig. 1A), whereas SH3TC2-HA co-localized with a plasma membrane marker (Na,K-ATPase) and also showed a perinuclear punctate pattern (Fig. 1B). If wild-type SH3TC2 was myristoylated, N-terminal tagging would disrupt this modification, and therefore the normal pattern would be the one observed with the HA tag. An alternative explanation would be that the difference could be due to the nature of the two tags. We confirmed the same results using a GFP tag: the N-terminally tagged protein had an identical localization to myc-SH3TC2 and the C-terminally tagged protein localizes like SH3TC2-HA (data not shown). These results clearly indicate that the nature of the tag is irrelevant, but its position is not.

Our observations suggest that (i) SH3TC2 is targeted to cellular membranes, including plasma membrane and cytoplasmic vesicles and (ii) this targeting requires myristoylation at its N terminus. We set out to prove these two points.

SH3TC2 co-localizes with components of the endocytic pathway

As we showed above, the SH3TC2-HA is co-localized with the Na,K-ATPase and also presented perinuclear localization in structures that resemble vesicles. To investigate the nature of these structures, we performed co-localization experiments using different antibodies for cytoplasmic organelles in COS-7 cells. Using well-described markers, we observed that SH3TC2 localizes to several components of the endocytic pathway. We found co-localization with the following markers (Fig. 1C–E and further examples in Supplementary Material, Fig. S2): EEA1, a marker of early endosomes which is present in a vesicular pattern; mannose-6-phosphate receptor (M6PR), found in late endosomes and *trans*-Golgi network (TGN); and clathrin heavy chain (CHC), which is involved in vesicular trafficking between the plasma membrane, endocytic pathway and the TGN. In contrast, SH3TC2-HA did not co-localize with antibodies labeling the endoplasmic reticulum (GRP94), peroxisomes (PMP70) or lysosomes (LAMP1) (Supplementary Material, Fig. S3).

SH3TC2 is tethered to cell membranes by N-myristoylation at glycine 2

To determine whether the localization of SH3TC2 required N-terminal myristoylation, we generated a construct which lacks the first five amino acids after methionine SH3TC2(Δ2-6). This truncated protein showed a diffuse cytoplasmic pattern which was very similar to the myc-tagged version (Fig. 2A). When we investigated its co-localization with all the organellar markers that are associated to wild-type SH3TC2, we found that it did not colocalize with any of them. Although the diffuse pattern of the mutant protein results in some overlap with most perinuclear structures (including the structures marked by M6PR and CHC), there is no specific co-localization in particular structures, such as the one observed with the wild-type (Fig. 2B–D, and further examples in Supplementary Material, Fig. S2). The glycine at position 2 starting from the start codon is absolutely necessary for the N-myristoylation of proteins (38). SH3TC2 contains glycines at positions 2 and 3, so to confirm that SH3TC2 needs to be myristoylated to reach its membrane localization, both glycines were independently mutated to alanine (p.G2A and p.G3A). As expected, p.G3A conserved the same pattern than the wild-type SH3TC2-HA (Figs 1B and 2E), whereas p.G2A showed an expression pattern which was undistinguishable from to SH3TC2(Δ2-6) and myc-SH3TC2 (Figs 1A and 2A, F).

To determine the degree of membrane association of SH3TC2, we performed a high speed centrifugation analysis. With this technique, soluble proteins are released in the supernatant, whereas membrane-associated proteins remain in the pellet. The strength of this membrane association is then tested by extraction with high salt and high pH conditions. Only proteins that are strongly associated will remain bound after these two treatments. Western blot analysis of the different fractions demonstrated that SH3TC2-HA was not present in the soluble fraction and that only a small amount of SH3TC2-HA was released with high pH, but not with high salt concentration (Fig. 3A). For comparison, we studied two of the proteins that co-localized with SH3TC2: the membrane-associated protein EEA1 is released into the soluble fraction, and the integral membrane protein

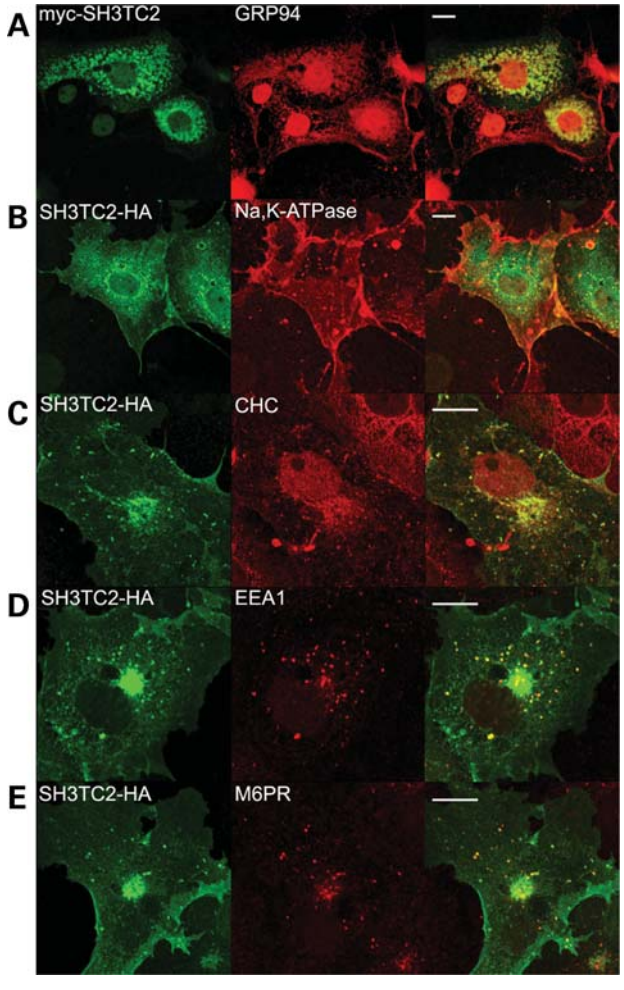

Figure 1. Sub-cellular localization of SH3TC2. COS-7 cells transfected with plasmids encoding myc-SH3TC2 (**A**) and SH3TC2-HA (**B**–**E**) were fixed and immunostained with anti-myc for myc-SH3TC2 (A) or anti-HA for SH3TC2-HA (B–E), and one of the following organellar markers: anti-GRP94 (A), anti-Na,K-ATPase (B), anti-CHC (C), anti-EEA1 (D), anti-M6PR (E). The myc and HA detections are shown in the green channel, and the organellar markers in the red channel, the overlay of both channels is shown in the right panel. The scale bar is 10 μm.

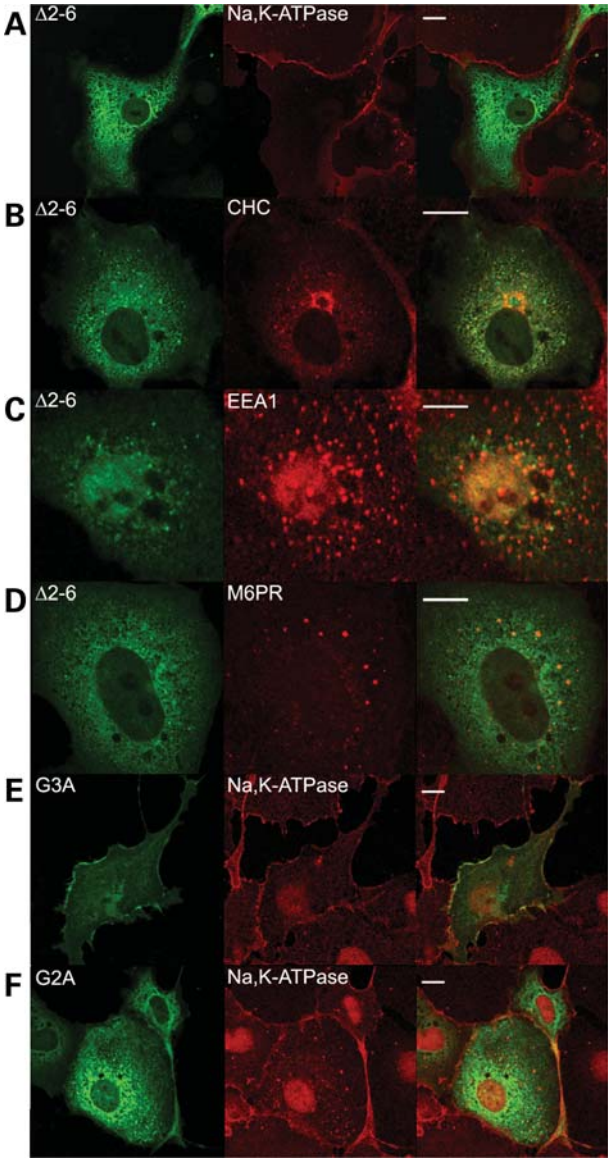

Figure 2. Effect of myristoylation on the localization of SH3TC2. COS-7 cells were transfected with a plasmids encoding the HA-tagged mutant proteins SH3TC2(Δ2-6) (**A**–**D**), SH3TC2(G3A) (**E**) or SH3TC2(G2A) (**F**). After fixation, the cells were immunostained with anti-HA to detect the mutant proteins and anti-Na,K-ATPase (A, E, F), anti-CHC (B), anti-EEA1 (C), anti-M6PR (D) for organelles. The anti-HA detection is shown in the green channel, the organellar markers in the red channel, and the overlay is show in the right panel. The scale bar is 10 μm.

Na,K-ATPase shows membrane association similar to SH3TC2. Therefore, we can conclude that SH3TC2 is strongly associated with cellular membranes. In contrast, part of SH3TC2(Δ2-6) was released into the soluble fraction. Still, about half of the protein remained membrane-bound indicating that association with membranes is not exclusively through myristoylation and could also be mediated by direct protein–protein interactions.

To obtain independent support for a plasma membrane localization of SH3TC2-HA, we prepared sub-cellular fractionation using sucrose gradient centrifugation. Western blot analysis of the fractions showed the presence of SH3TC2 in the plasma membrane fraction obtained from COS-7 (Fig. 3B) or HeLa cells (data not shown). The strongest band of SH3TC2 overlaps with the strongest band of Na,K-ATPase and caveolin-1, this last also associated with lipid rafts.

The possible association of SH3TC2 with lipid rafts is an interesting possibility, given that its plasma membrane localization is not homogeneous and seems to be enriched in certain areas. To investigate the presence of SH3TC2 in lipid rafts, we transfected COS-7 cells with SH3TC2-HA and processed the membrane pellet by a flotation gradient experiment. With this technique, proteins associated with lipid rafts are recovered mainly in the lightest density fractions. Western blot analysis showed that a small amount of SH3TC2-HA is released in the lowest density fractions, corresponding to the purified lipid rafts (Fig. 3C, lanes 1 and 2). As expected, caveolin-1 was accumulated in the low-density fractions. This finding indicates that at least part of the SH3TC2-HA protein is associated with these membrane domains.

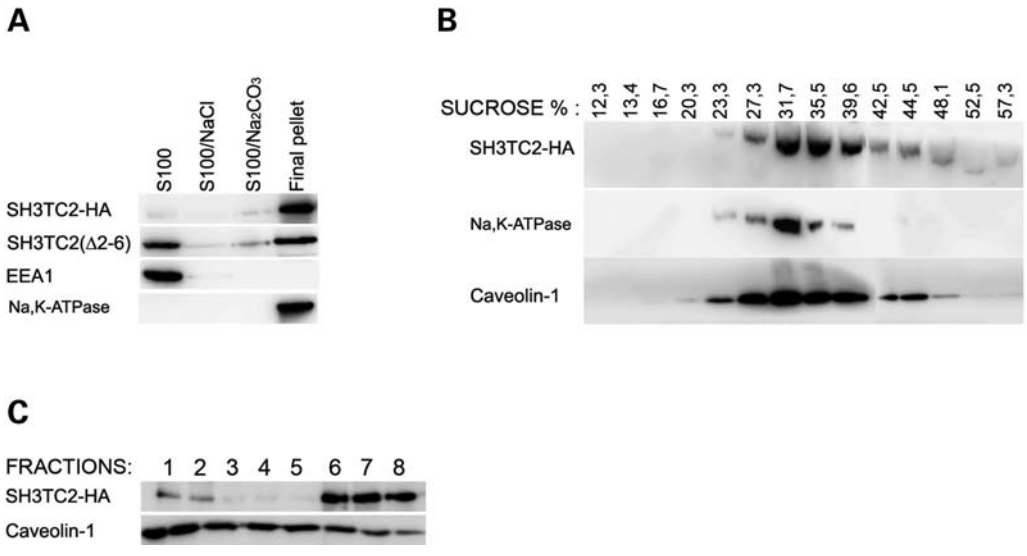

Figure 3. SH3TC2 is strongly associated with cellular membranes. For each experiment, COS-7 cells were transfected with plasmid encoding HA-tagged versions of SH3TC2 (**A**–**C**) and SH3TC2(Δ2-6) (**A**). (A) Cell lysates were centrifuged at 100 000*g* to produce soluble fraction (S100). The membrane-associated pellet was sequentially extracted with high salt buffer (S100/NaCl), high pH buffer (S100/Na_2CO_3), and the final pellet was solubilized with RIPA buffer. Equal extractions were separated by SDS–PAGE and analyzed by western blotting with anti-HA, anti-EEA1 or anti-Na,K-ATPase. (B) To study membrane association of SH3TC2-HA crude membrane extracts were fractionated in a sucrose gradient and analyzed by western blotting with anti-HA for the detection of SH3TC2-HA, anti-Na,K-ATPase and anti-Caveolin-1. Above each fraction, the percentage of sucrose is indicated. (C) Flotation gradient fractions collected from lowest (lane 1) to highest density (lane 8). SH3TC2-HA was detected with anti-HA, and Caveolin-1 was detected with anti-Caveolin-1.

The SH3 and TPR domains are also involved in anchoring SH3TC2 to the cell membranes

The previous results demonstrated that SH3TC2 is strongly associated with membranes and that SH3TC2 needs to be myristoylated to efficiently localize to cellular membranes, but they also disclosed association with membranes in the absence of myristoylation. To understand other requirements for the anchoring of SH3TC2 protein, we generated a series of constructs containing engineered deletions (Fig. 4A). A truncated protein lacking all SH3 and TPR domains, conserving only the first 180 amino acids (ΔSH3ΔTPRs) did not co-localize with plasma membrane (Fig. 4B) nor with *trans*-Golgi vesicles (Fig. 4C), but presented a cytoplasmic localization with a punctate pattern that co-localized weakly with both early and late endosomes (Supplementary Material, Fig. S4A and B). Deletion of either the two SH3 domains (ΔSH3) or the C-terminal TPR domains (ΔTPR) did not affect normal localization (Fig. 4D–G; Supplementary Material, Fig. S4C–H). Occasionally, SH3TC2(ΔTPR) presented the same punctate pattern as SH3TC2(ΔSH3ΔTPR). This result suggests that either SH3 or TPR domains in combination with myristoylation are sufficient to anchor SH3TC2 protein to the plasma membrane and all the vesicular structures where the wild-type protein is found. Both types of domain probably achieve this by mediating interactions with other proteins.

Plasma membrane localization is altered by SH3TC2 missense mutations

We have shown that SH3TC2 is associated with components of the endocytic pathway through myristoylation and protein interactions mediated by the SH3 and TPR domains. We wondered if these findings may help to explain the pathogenicity of known *SH3TC2* mutations. To this end, we tested the effect of disease-associated *SH3TC2* mutations on protein localization in COS-7 cells. For this, we decided to use the following mutations (Fig. 5A): (i) mutations that generate stop codons and truncated proteins: p.C737_P738delinsX and p.R1109X, the two mutations found in the Gypsy population, and p.R954X observed as a founder mutation in French-Canadians and present in other Caucasian populations; (ii) missense mutations: p.R529Q causative of intermediate phenotype, p.E657K and p.R658C two neighboring mutations expressed as a typical phenotype and p.A758D the unique mutation identified in a patient with evident demyelinating CMT (39).

All three premature termination codon mutations and the missense mutation p.A758D showed the same pattern as the wild-type SH3TC2-HA (data not shown). However, the remaining three missense mutations displayed some differences with the localization of the canonical SH3TC2. p. R529Q had a variable pattern. In some cells, its distribution was similar to the wild-type, but a high proportion of cells showed abnormal localization. Most cells showed strong reduction or absence from the plasma membrane, in fact we did not find co-localization with Na,K-ATPase (Fig. 5B). Co-localization with CHC (Fig. 5C) showed a variable cellular localization in the *trans*-Golgi, but more striking complete absence from cytoplasmic endosomes (Fig. 5D and E). A similar pattern, although slightly less severe, was observed for p.E657K (Fig. 5F–I) and p.R658C (Supplementary Material, Fig. S5) mutations. The similarity in the localization pattern of these three mutant proteins seems to indicate that the region comprising the first-TPR domain is important for the localization of SH3TC2. To investigate this, we generated a construct that included only the region of the first-TPR

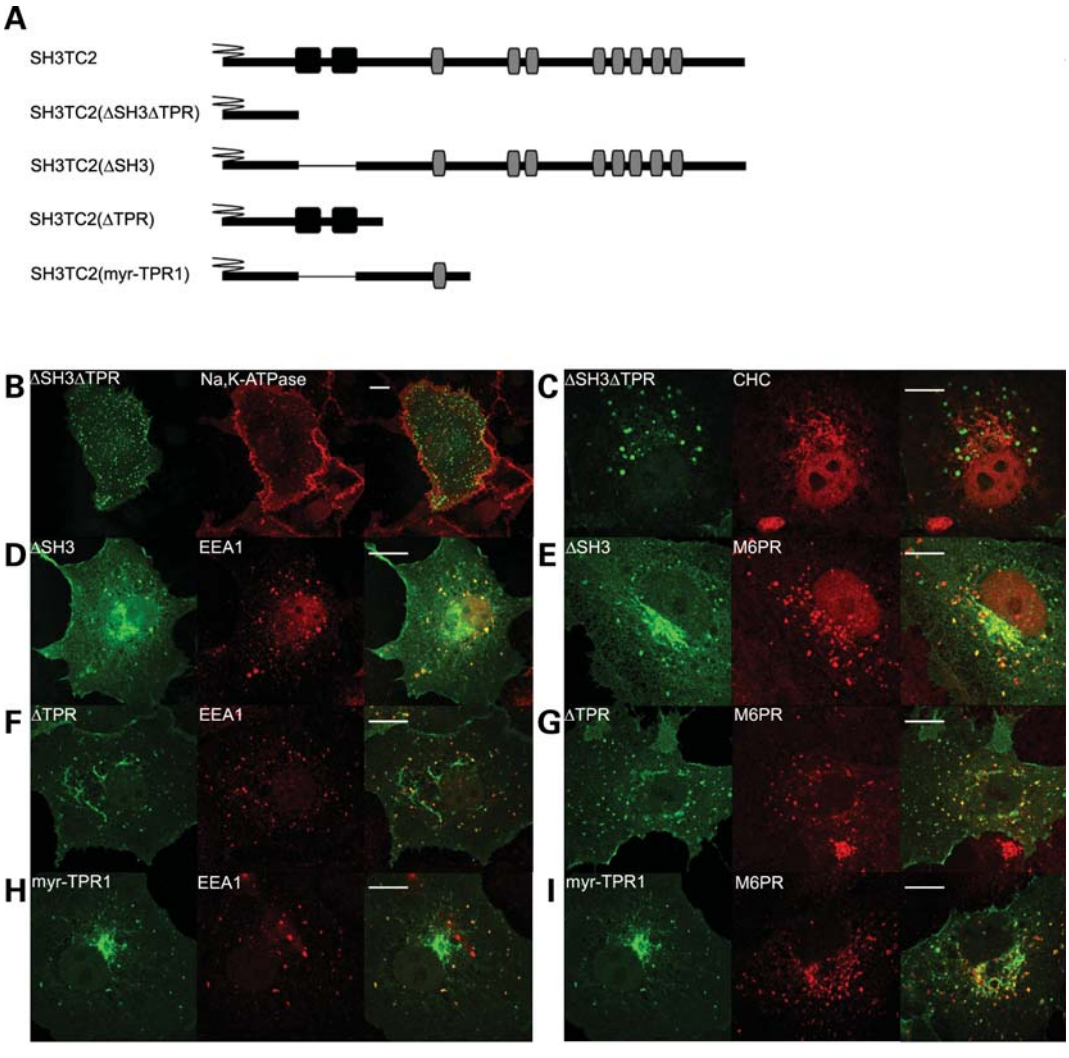

Figure 4. The SH3 and TPR domains are required for association with membranes. (**A**) Schematic representation of SH3TC2 mutated constructs. Black squares represent SH3 domains, gray ovals TPR domains, broken lines mark myristoylation motifs, and thin lines represent internal deletions. All these forms are HA-tagged at the C-terminus. (**B**–**I**) Effect of the different deletions on the localization of the protein. COS-7 cells were transfected with plasmids encoding SH3TC2(ΔSH3ΔTPR) (B, C), SH3TC2(ΔSH3) (D, E), SH3TC2(ΔTPR) (F, G) or SH3TC2(Myr-TPR1) (H, I). After fixation, the cells were immunostained with anti-HA (B–I) and one of the following organellar markers: anti-Na,K-ATPase (B), anti-CHC (C), anti-EEA1 (D, F, H), anti-M6PR (E, G, I). The detection of HA is shown in the green channel, the detection of the organellar markers in the red channel, with the overlay of both channels in the right panel. The scale bar is 10 μm.

domain fused to the N terminus and excluded any other SH3 and TPR domains (myr-TPR1, Fig. 4A). This extremely streamlined version of the protein can still localize to the same structures as the complete wild-type protein (Fig. 4H–I; Supplementary Material, Fig. S4G–H). Therefore, the first-TPR repeat is necessary for the proper cell localization and/or function of SH3TC2.

DISCUSSION

CMT disease is an extremely heterogeneous disease, both at the clinical and at the genetic levels. To date, 26 genes have been found to be associated with CMT and they encode proteins with a broad spectrum of functions. CMT4C is caused by mutations in the *SH3TC2* gene (3). As a first step to understand the pathogenesis of CMT4C, we have investigated the intracellular localization of SH3TC2 in a cell culture system. As we do not have an antibody that can recognize the protein, we have labeled the coding sequence of SH3TC2 with a non-disruptive peptide tag. Our results have disclosed that SH3TC2 is located to structures of the endocytic pathway, namely clathrin-coated vesicles, including the TGN, early endosomes and late endosomes, and discrete domains of the plasma membrane. Analysis of the SH3TC2 sequence revealed a putative N-myristoylation signal. N-myristoylation is a co-translational modification in which the start methionine is removed and a myristate is linked to glycine 2 (38). Proteins with myristate are able to interact reversibly with other proteins as well as cellular membranes (40). Through immunofluorescent localization in cells and biochemical tests using wild-type and mutated versions of SH3TC2, we have shown

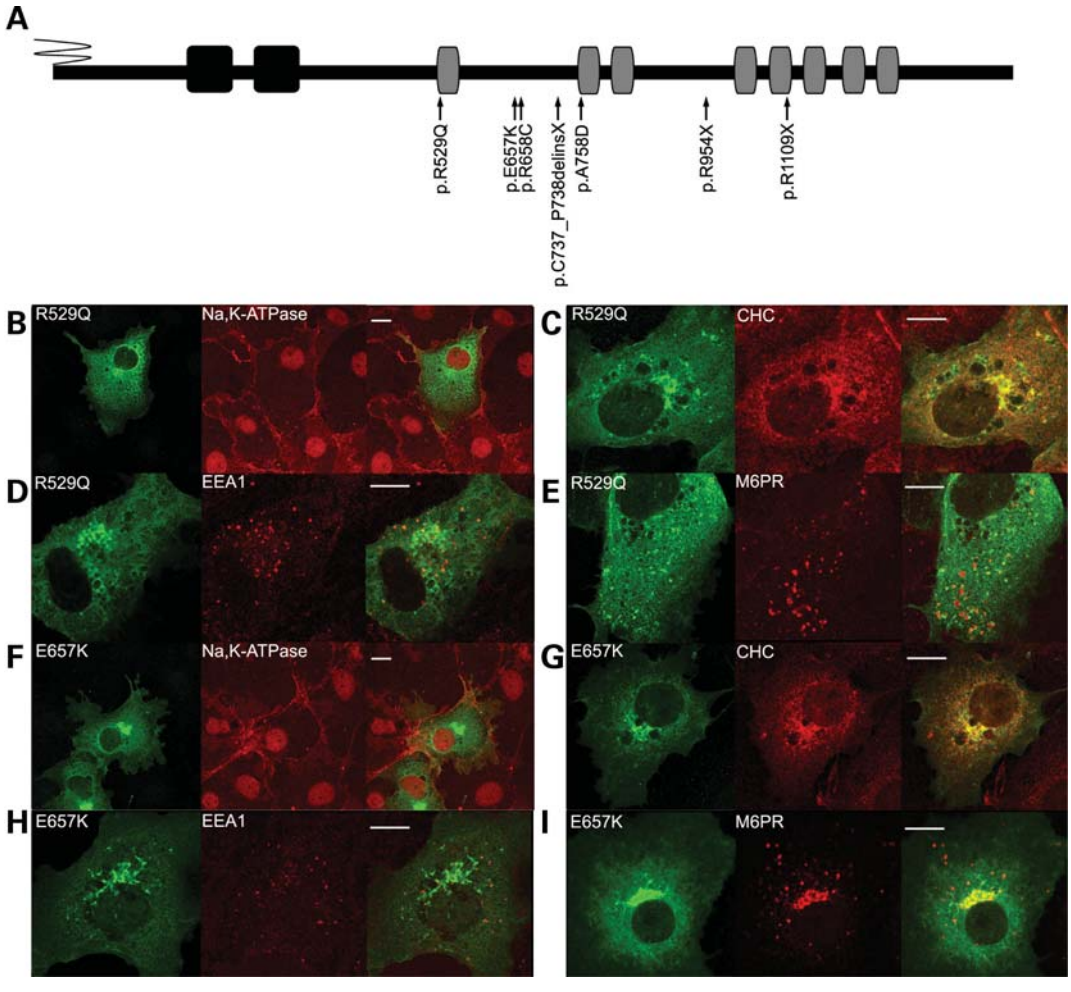

Figure 5. (**A**) Schematic representation of clinical missense and nonsense mutations (black arrows) on SH3TC2. The SH3TC2 protein is represented as in Figure 4. (**B**–**I**) Effect of the mutations p.R529Q (B–E) and p.E657K (F–I) on SH3TC2 localization. These proteins are HA-tagged and were detected by an anti-HA antibody (green channel). In addition, anti-Na,K-ATPase (B, F), anti-CHC (C, G), anti-EEA1 (D, H) and anti-M6PR (E, I) were used as markers (red channel). The overlay is shown in the right panel. The scale bar is 10 μm.

that this protein is strongly associated with cell membranes: it is purified in membrane-containing fractions and its association is resistant to high salt and high pH extractions. At least some of the protein present in the plasma membrane is associated with lipid rafts. To achieve this strong membrane association, myristoylation is required. When myristoylation is prevented, the protein loses its membrane localization and appears associated with the endoplasmic reticulum, where some misfolded or mutant proteins are targeted for degradation. Western blot analysis of membrane fractionation showed that even in the absence of myristoylation, some protein is still bound to membranes. This observation suggests that other domains of SH3TC2 may be involved in localization.

SH3TC2 receives its name because of the presence of two types of domains: SH3 and TPR (3). These are prime suspects as mediators for the localization of SH3TC2, as both domain families are involved in protein–protein interactions. SH3 domains participate in the binding to proline-rich regions in other proteins, and TPR domains, usually present in tandem repeats, mediate protein–protein binding and multiprotein complex formation in many different contexts (41–44). An N-terminal protein fragment containing the N-myristoylation motif, but lacking SH3 and TPR motifs was not able to maintain the cellular localization of the wild-type SH3TC2. In contrast, deletion of either the SH3 or the TPR domains only had no effect in protein localization, indicating that myristoylation and the presence of one of these domain families was sufficient to target the protein to its proper location. Most striking, a construct containing only the N terminus and just the first-TPR motif is able to localize normally. These observations suggest that probably both the SH3 and the TPR domains mediate interactions of SH3TC2 with other proteins. SH3 domains have been described to be involved in different instances of clathrin-mediated vesicle endocytosis, including synaptic vesicle recycling (reviewed in 45, 46).

The endosomal protein sorting is a complex and highly dynamic process in which proteins are transported, recycled and degraded, according to their allocated fate. This process can be both regulated and constitutive. The endosomal compartments consist of early endosomes that can be subdivided into sorting endosomes (SEs) and recycling endosomes, late

endosomes and lysosomes (47). The SEs can have three different destinations: the plasma membrane, the TGN and the lysosomes (47). In addition, there is a bi-directional traffic between the endosomes and TGN (47–49). There is a clear link between known CMT proteins and the process of endocytosis, and sorting from the *trans*-Golgi to the endocytic compartments (50). These include membrane trafficking regulators such as the MTMR2 and MTMR13 myotubularins (51), the GTPases DNM2 (28) and Rab7 (52) and the ubiquitin ligase LITAF (24). Some other important CMT proteins are among the cargo to be carried by the endocytic and sorting system, mainly the myelin components MPZ and PMP22. In the most prevalent form of CMT, CMT1A, caused by the *PMP22* duplication, it has been observed that at least part of the pathology is due to alterations in intracellular trafficking and degradation of membrane proteins caused by the overexpression of PMP22 protein (53). We have established that SH3TC2 is located in some of the components of the endocytic pathway, in a fashion that is dependent on myristoylation and protein interactions mediated by SH3 and TPR domains. At this stage, we cannot determine whether it participates in the trafficking machinery or whether it is dependent on this machinery to reach its destination.

Our main goal is to understand the pathogenesis of CMT4C. To this end, we decided to study some disease-associated mutations. Three of the missense mutations, p.R529Q, p.E657K and p.R658C, are clustered around the first-TPR domain, whereas a fourth one, p.A758D, is downstream of these. Interestingly, the first three mutations have an effect on protein localization. This effect is variable, but in the most extreme cases implies an important reduction in plasma membrane localization and a complete absence from cytoplasmic vesicles of all types where SH3TC2 is normally present. As for the TGN domain, we observed a variable perinuclear location for p.R529Q, and a strong retention of perinuclear location in the cases of p.E657K and p.R658C, which co-localized with clathrin-coated pits of the TGN. These observations suggest that the region of the first-TPR domain is essential for the localization of the protein. This conclusion is reinforced by our observation that a construct with the N-terminal portion and the first-TPR domain can localize correctly. Still, we cannot discount that the effects of these mutations go beyond protein localization and may alter function as well. In comparison with the other three missense mutations, it is striking that the p.A758D mutation does not alter the cellular localization of SH3TC2. This change was identified in a sporadic case with a demyelinating CMT form and a second disease-causative mutation has not been found in the *SH3TC2* gene (39). Mutations in other CMT genes (*PMP22*, *MPZ*, *GJB1*, *GDAP1*, *SIMPLE* and *EGR2*) were also excluded. The *SH3TC2* p.A758D mutation was screened in 101 healthy individuals and was not detected providing additional support that this change could be pathological. However, in the light of our results, it is possible that it is a polymorphism, and mutations in an as yet unidentified CMT gene are responsible for the disease.

In contrast, none of the three nonsense mutations (p.C737_P738delinsX, p.R954X and p.R1109X) showed any alteration in localization when compared with the wild-type. This result is not surprising, since our engineered construct lacking the C-terminal half of the protein was localized correctly. We assayed these proteins through directed mutagenesis of cDNAs, but in their native context, the mutant transcripts are probably degraded by the nonsense-mediated mRNA decay pathway. Therefore, the issue of whether they can be correctly localized or not is probably irrelevant for the pathogenesis of CMT4C.

The dynamic communication between Schwann cells and axons is fundamental for the correct function of the peripheral nerve. Nerve biopsies from CMT4C patients show demyelinated fibers that are usually surrounded by basal lamina onion bulbs (6). As we have discussed above, several CMT proteins are involved in endocytosis and trafficking of membrane components from the TGN to the endocytic compartments. These proteins are relevant for the maintenance and formation of the myelin (50). In addition, endocytosis is strongly implicated in the regulation of signal transduction (54). We propose that SH3TC2 is a relevant protein of the Schwann cell physiology and molecular defects of this protein could alter its proper function in the endocytic pathway causing demyelinating neuropathy.

MATERIAL AND METHODS

Patients

Our clinical series comprise 177 Caucasian non-Gypsy patients who suffer from CMT, supervised at the Neurology Service of the University Hospital La Fe. Diagnostic criteria for demyelinating CMT were median NCV under 38 m/s and nerve fiber demyelination with proliferation of Schwann cells forming 'onion bulbs'. Patients with NCV between 30 and 40 m/s and nerve pathology with both axonal and demyelinating features or undefined were classified as intermediate CMT. Eighty-eight probands were diagnosed with a demyelinating neuropathy and two patients with an intermediate form. A previous mutational screening of the CMT genes *PMP22* (CMT1A duplication and point mutations), *MPZ*, *GJB1*, *GDAP1*, *SIMPLE*, *NEFL*, *EGR2*, *PRX* and *FIG4*, allowed us to identify the causative mutations in 77 patients with demyelinating features. The remaining 11 probands and the two patients with an intermediate form were included in a search for mutations in the *SH3TC2* gene. In addition, we included in this study a patient (ID no. 744) for whom a clinical diagnosis of CMT4C was suspected whose sample was sent to us to perform a genetic test. The series was distributed as follows: ten simplex and four multiplex families. All patients and relatives were aware of the investigative nature of the studies and gave their consent.

Mutation screening of the *SH3TC2* gene

The 17 exons of the *SH3TC2* gene and their flanking intronic sequences were amplified using primers as described elsewhere (3). Mutation screening was performed by Denaturing High Performance Liquid Chromatography (DHPLC; Transgenomic WAVE, Inc., San José, CA, USA) and those PCR products showing anomalous DHPLC patterns were sequenced in an ABI Prism 3130×l autoanalyser (Applied Biosystems,

Foster City, CA, USA). Sequence alignment and analysis were carried out with the BLAST program (55).

Cloning of *SH3TC2*

The full-length *SH3TC2* transcript contains an ORF of 1288 codons (3) and the corresponding protein contains two SH3 domains and eight TPR domains (SwissProt Q8TF17). To obtain a cDNA with the same coding region, we proceeded as follows. We amplified a 3344 bp fragment by PCR on a human brain cDNA library (cat.10410-010 Invitrogen, Carlsbad, CA, USA), which comprises from position 565 from the start codon, within exon 6, to the 3′-UTR region (forward primer 5′-ccaccagccgagaaggaagg-3′, reverse primer 5′-agtctggccatgccaaatgtcc-3′). This fragment was cloned into the pGEM-T vector (Promega, Madison, WI, USA) resulting in plasmid pGEM-T::3344. The N-terminal region from the start codon to position 564 was obtained from two image clones (GeneService Ltd, UK). The first IMAGE clone (ID: 6048901) contained from the 5′-UTR to exon 5. The second (ID: 6055718) contained from the exon 1 (at position 43 from ATG codon) to the exon 8 region. A *Bpi*I–*Bam*HI restriction fragment was eliminated from the second clone and substituted by with a *Bpi*I–*Bam*HI from the first clone, thus obtaining an uninterrupted ORF from the start codon through to exon 8. To generate the full length ORF, a *Sac*II–*Bsm*I fragment from this hybrid sequence containing the N-terminal portion was cloned into pGEM-T::3344 digested with the same enzymes (pGEM-T::SH3TC2).

We performed an *in silico* analysis of the human SH3TC2 protein Q8TF17 using the protein knowledgebase UniProtKB (http://www.uniprot.org) and the PSORT II software (http ://psort.ims.u-tokyo.ac.jp).

Plasmid construction and site-directed mutagenesis

For the synthesis of the tagged versions of *SH3TC2* (SH3TC2-GFP, GFP-SH3TC2, SH3TC2-HA and myc-SH3TC2), the coding sequence of *SH3TC2* was first amplified by PCR from pGEM-T::SH3TC2. For each construct, a pair of primers was designed, containing adapters with restriction sites that allowed in-frame cloning in the relevant vector. These vectors were pEGFP-C1, pEGFP-N1 and pCMV-myc from Clontech (Mountain View, CA, USA), and pcDNA3-HA, a vector derived from the Invitrogen pcDNA3 kindly donated by D. Barettino. The sequences for the primers used for the synthesis of each one of these constructs are given in Supplementary Material, Table S1.

The SH3TC2-HA constructs carrying the mutations Δ2-6, ΔSH3ΔTPRs and ΔTPR were made by inserting the sequence of interest, amplified from the pGEM-T::SH3TC2 plasmid by PCR, into the pcDNA3-HA vector, resulting in the corresponding defective ORFs fused to a C-terminal HA tag. The primer sequences are given in Supplementary Material, Table S1.

The ΔSH3 mutation was generated in two segments, N-terminal and C-terminal to the SH3 domains, respectively. Each segment was obtained by PCR from pGEM-T::SH3TC2 (primer sequences in Supplementary Material, Table S1). Then, a *Kpn*I–*Eco*RI fragment from the N-terminal amplicon and an *Eco*RI–*Eco*RV fragment from the second one were sequentially cloned into the pcDNA3-HA vector backbone. Any mutations introduced as a consequence of including the restriction site were removed by site-directed mutagenesis as described below. The resulting plasmid was pcDNA3-HA::ΔSH3. The myr-TPR1 segment was obtained by amplification from pcDNA3-HA::ΔSH3 plasmid by PCR into the same vector pcDNA3-HA.

The SH3TC2 variants p.G2A and p.G3A and the disease-associated mutations (p.R529Q, p.E657K, p.R658C, p. C737_P738delinsX, p.A758D, p.R954X and p.R1109X) were generated by site-directed mutagenesis with specific primers containing the nucleotide changes and following the instruction manual from QuickChangeTM Site-Directed Mutagenesis kit (Stratagene). The sequences of all the constructs were confirmed by automated DNA sequencing in an ABI Prism 3130XL autoanalyser (Applied Biosystems).

Cell culture, immunocytochemistry and microscopy

COS-7 or HeLa cells were grown in a humidified incubator with 5% CO_2 at 37°C in DMEM containing 10% (v/v) fetal bovine serum (FBS) supplemented with 2 mM glutamine, 100 IU/ml penicillin and 100 μg/ml streptomycin (Invitrogen). To carry out the protein expression and co-localization analysis, 100 000 COS-7 or 200 000 HeLa cells were cultured in six-well plates on glass coverslips. Next day, when they reached 70–80% confluency, we transfected them with the CAPHOS kit (Sigma-Aldrich, St Louis, MO, USA) using 5 μg of plasmidic DNA. We used lipofectamine (Roche) for HeLa cells, using a ration of 5 μl lipofectamine for each 2 μg of plasmid DNA. Western blot analysis was performed after transfection of each construct to test the integrity of the expressed protein and to ensure that the different constructs were expressed at similar levels.

For co-localization studies, cells were fixed and processed for immunofluorescence microscopy 24 h post-transfection. Briefly, cells were fixed in 4% (w/v) paraformaldehyde in phosphate-buffered saline (PBS) for 15 min or in methanol for 20 min at −20°C, permeabilized in 0.5% (w/v) Triton X-100 in PBS for 30 min, blocked with 10% (v/v) FBS/0.1% (w/v) Triton X-100/0.5% (w/v) BSA in PBS for 1 h and then probed with primary antibodies diluted in blocking solution. The following primary antibodies were used: mouse monoclonal anti-Na,K-ATPase for plasma membrane (Abcam, Cambridge, UK; used at 1:100); rabbit polyclonal anti-GRP94 (Abcam; used at 1:100) for endoplasmic reticulum; mouse monoclonal anti-CHC for clathrin-coated vesicles (BD Biosciences, San Jose, CA, USA, used at 1:50); mouse monoclonal anti-EEA1 for early endosomes (BD Biosciences; used at 1:100); mouse monoclonal anti-M6PR for late endosomes (Abcam; used at 1:250); polyclonal rabbit anti-PMP70 for peroxisomes (Invitrogen; used at 1:100), anti-LAMP1 clone H4A3 for lysosomes (developed by J. Thomas August and James E.K. Hildreth, obtained from the Developmental Studies Hybridoma Bank, University of Iowa; used at 1:30). The secondary antibodies used were goat anti-mouse or goat anti-rabbit immunoglobulins coupled to Alexa Fluor 488 or Alexa Fluor 633 (Invitrogen; used at 1:250). The samples were mounted in Fluoromount-G

(Southern Biotech, Birmingham, AL, USA). Cells were examined using a Leica DM RXA2 microscope and Leica TCS SP Confocal System. Images were manipulated and analyzed with the Leica Confocal Software and the ImageJ suite.

Membrane fractionation, lipid raft purification

To perform crude membrane preparation and the subsequent sucrose gradient fractionation from COS-7 or HeLa cells, we used previously described procedures (56) with minor modifications. Details are available upon request.

To analyze the possible interaction of SH3TC2-HA with membranes, we performed a high-speed centrifugation analysis. COS-7 cells transfected with pCDNA3-HA-SH3TC2 were scraped from 100 mm dishes 24 h after transfection and washed twice with PBS. The cells were then resuspended in 1 ml of lysis buffer (10 mM Tris–HCl pH 7.4, 2.5 mM $MgCl_2$, protease inhibitors) and transferred to ice for 15 min. Cells were lysed with 25–40 strokes of a dounce homogenizer and the lysate was gently layered over a sucrose cushion (0.5 M sucrose, 10 mM Tris–HCl pH 7.4, 2.5 mM $MgCl_2$). Nuclei and debris were discarded by centrifugation at 5000*g* for 10 min at 4°C. The upper layer consisting of cytoplasmic extract was collected and was centrifuged at 100 000*g* for 1 h in a MLA-130 rotor (Beckmann), resulting in a soluble supernatant and pellet containing membranes and membrane-associated proteins. The pellet was resuspended in 100 μl of high-salt buffer (10 mM Tris–HCl pH 7.4, 750 mM NaCl, with protease inhibitors) and centrifuged for 1 h at 100 000*g* yielding a high-salt supernatant and pellet. This pellet was then resuspended in 100 μl of high pH buffer (10 mM Tris–HCl pH 7.4, 100 mM Na_2CO_3, with protease inhibitors) and centrifuged for 1 h at 100 000*g* yielding a high pH supernatant and final pellet. The final pellet was resuspended in 100 μl of RIPA buffer (50 mM Tris–HCl pH 7.4, 5 mM DTT, 150 mM NaCl, 1% NP-40, 0.5% deoxycholate). Equal cell equivalents were resolved by SDS–PAGE and the relevant proteins were detected by western blot analysis.

Flotation gradients to purify raft proteins were also performed with COS-7 24 h post-transfection. The cell pellet was lysed in 500 μl of TNE buffer (50 mM Tris–HCl pH 7.4, 150 mM NaCl, 5 mM EDTA, with protease inhibitors) by 25–40 strokes of a dounce homogenizer. After discarding the unbroken cells and debris, the clear lysate was incubated with Triton X-100 (1% final) for 30 min on ice. After the extraction with Triton X-100, the lysate (400 μl) was adjusted to 40% Optiprep by adding 800 μl of Optiprep solution (Sigma-Aldrich) and overlaid with 2.4 ml of 30% Optiprep in TXNE (TNE, 0.1% Triton X-100) and 400 μl of TXNE. The samples were centrifuged at 164 000 g for 18 h in a SW60Ti rotor (Beckmann). Fractions were collected from the top, precipitated by adding two volumes of 15% trichloracetic.

All samples were analyzed by SDS/PAGE and western blotting. To perform western blot analysis, the following antibodies were used: rabbit polyclonal anti-HA (Sigma-Aldrich; used at 1:1000), mouse monoclonal anti-Na,K-ATPase (Abcam; used at 1:1000), rabbit polyclonal anti-Caveolin-1 (Santa Cruz Biotechnology, Santa Cruz, CA, USA; used at 1:1000) and mouse monoclonal anti-EEA1 for early endosomes (BD Biosciences; used at 1:1000).

SUPPLEMENTARY MATERIAL

Supplementary Material is available at *HMG* online.

ACKNOWLEDGEMENTS

We are grateful to patients and their families for their kind collaboration. We thank B. Alarcón for his technical assistance and also anonymous reviewers for their invaluable insight and suggestions.

Conflict of Interest statement. None declared.

FUNDING

This work was supported by the Fondo de Investigación Sanitaria [grant numbers PI08/90857, PI08/0889, CP08/00053] and the Spanish Ministry Science and Innovation [grant number SAF2006-01047]. V.L. is a recipient of JAE predoctoral fellowship from the Spanish Scientific Research Council (CSIC). M.I.G. has a 'Ramón y Cajal' contract funded by the Ministry of Science and Innovation. C.E. has a 'Miguel Servet' contract funded by the Fondo de Investigación Sanitaria. Both CIBERER and CIBERNED are initiatives from the Instituto de Salud Carlos III.

REFERENCES

1. Skre, H. (1974) Genetic and clinical aspects of Charcot-Marie-Tooth's disease. *Clin. Genet.*, **6**, 98–118.
2. Combarros, O., Calleja, J., Polo, J.M. and Berciano, J. (1987) Prevalence of hereditary motor and sensory neuropathy in Cantabria. *Acta Neurol. Scand.*, **75**, 9–12.
3. Senderek, J., Bergmann, C., Stendel, C., Kirfel, J., Verpoorten, N., De Jonghe, P., Timmerman, V., Chrast, R., Verheijen, M.H., Lemke, G. *et al.* (2003) Mutations in a gene encoding a novel SH3/TPR domain protein cause autosomal recessive Charcot-Marie-Tooth type 4C neuropathy. *Am. J. Hum. Genet.*, **73**, 1106–1119.
4. Azzedine, H., Ravise, N., Verny, C., Gabreels-Festen, A., Lammens, M., Grid, D., Vallat, J.M., Durosier, G., Senderek, J., Nouioua, S. *et al.* (2006) Spine deformities in Charcot-Marie-Tooth 4C caused by *SH3TC2* gene mutations. *Neurology*, **67**, 602–606.
5. Gosselin, I., Thiffault, I., Tetreault, M., Chau, V., Dicaire, M.J., Loisel, L., Emond, M., Senderek, J., Mathieu, J., Dupre, N. *et al.* (2008) Founder SH3TC2 mutations are responsible for a CMT4C French-Canadians cluster. *Neuromuscul. Disord.*, **18**, 483–492.
6. Houlden, H., Laura, M., Ginsberg, L., Jungbluth, H., Robb, S.A., Blake, J., Robinson, S., King, R.H. and Reilly, M.M. (2009) The phenotype of Charcot-Marie-Tooth disease type 4C due to SH3TC2 mutations and possible predisposition to an inflammatory neuropathy. *Neuromuscul. Disord.*, **19**, 264–269.
7. Claramunt, R., Sevilla, T., Lupo, V., Cuesta, A., Millan, J.M., Vilchez, J., Palau, F. and Espinos, C. (2007) The p.R1109X mutation in SH3TC2 gene is predominant in Spanish Gypsies with Charcot-Marie-Tooth disease type 4. *Clin. Genet.*, **71**, 343–349.
8. Gooding, R., Colomer, J., King, R., Angelicheva, D., Marns, L., Parman, Y., Chandler, D., Bertranpetit, J. and Kalaydjieva, L. (2005) A novel Gypsy founder mutation, p.Arg1109X in the CMT4C gene, causes variable peripheral neuropathy phenotypes. *J. Med. Genet.*, **42**, e69.
9. Reilly, M.M. (2005) Axonal Charcot-Marie-Tooth disease: the fog is slowly lifting!. *Neurology*, **65**, 186–187.

10. Lupski, J.R., de Oca-Luna, R.M., Slaugenhaupt, S., Pentao, L., Guzzetta, V., Trask, B.J., Saucedo-Cardenas, O., Barker, D.F., Killian, J.M., Garcia, C.A. *et al.* (1991) DNA duplication associated with Charcot-Marie-Tooth disease type 1A. *Cell*, **66**, 219–232.
11. Fortun, J., Go, J.C., Li, J., Amici, S.A., Dunn, W.A. Jr and Notterpek, L. (2006) Alterations in degradative pathways and protein aggregation in a neuropathy model based on PMP22 overexpression. *Neurobiol. Dis.*, **22**, 153–164.
12. Filbin, M.T., Walsh, F.S., Trapp, B.D., Pizzey, J.A. and Tennekoon, G.I. (1990) Role of myelin P0 protein as a homophilic adhesion molecule. *Nature*, **344**, 871–872.
13. Bergoffen, J., Scherer, S.S., Wang, S., Scott, M.O., Bone, L.J., Paul, D.L., Chen, K., Lensch, M.W., Chance, P.F. and Fischbeck, K.H. (1993) Connexin mutations in X-linked Charcot-Marie-Tooth disease. *Science*, **262**, 2039–2042.
14. Bondurand, N., Girard, M., Pingault, V., Lemort, N., Dubourg, O. and Goossens, M. (2001) Human Connexin 32, a gap junction protein altered in the X-linked form of Charcot-Marie-Tooth disease, is directly regulated by the transcription factor SOX10. *Hum. Mol. Genet.*, **10**, 2783–2795.
15. Nagarajan, R., Svaren, J., Le, N., Araki, T., Watson, M. and Milbrandt, J. (2001) EGR2 mutations in inherited neuropathies dominant-negatively inhibit myelin gene expression. *Neuron*, **30**, 355–368.
16. Inoue, K., Khajavi, M., Ohyama, T., Hirabayashi, S., Wilson, J., Reggin, J.D., Mancias, P., Butler, I.J., Wilkinson, M.F., Wegner, M. *et al.* (2004) Molecular mechanism for distinct neurological phenotypes conveyed by allelic truncating mutations. *Nat. Genet.*, **36**, 361–369.
17. Warner, L.E., Mancias, P., Butler, I.J., McDonald, C.M., Keppen, L., Koob, K.G. and Lupski, J.R. (1998) Mutations in the early growth response 2 (EGR2) gene are associated with hereditary myelinopathies. *Nat. Genet.*, **18**, 382–384.
18. de Brito, O.M. and Scorrano, L. (2008) Mitofusin 2 tethers endoplasmic reticulum to mitochondria. *Nature*, **456**, 605–610.
19. Pedrola, L., Espert, A., Valdes-Sanchez, T., Sanchez-Piris, M., Sirkowski, E.E., Scherer, S.S., Farinas, I. and Palau, F. (2008) Cell expression of GDAP1 in the nervous system and pathogenesis of Charcot-Marie-Tooth type 4A disease. *J. Cell Mol. Med.*, **12**, 679–689.
20. Pedrola, L., Espert, A., Wu, X., Claramunt, R., Shy, M.E. and Palau, F. (2005) GDAP1, the protein causing Charcot-Marie-Tooth disease type 4A, is expressed in neurons and is associated with mitochondria. *Hum. Mol. Genet.*, **14**, 1087–1094.
21. Niemann, A., Ruegg, M., La Padula, V., Schenone, A. and Suter, U. (2005) Ganglioside-induced differentiation associated protein 1 is a regulator of the mitochondrial network: new implications for Charcot-Marie-Tooth disease. *J. Cell Biol.*, **170**, 1067–1078.
22. Moriwaki, Y., Begum, N.A., Kobayashi, M., Matsumoto, M., Toyoshima, K. and Seya, T. (2001) Mycobacterium bovis Bacillus Calmette-Guerin and its cell wall complex induce a novel lysosomal membrane protein, SIMPLE, that bridges the missing link between lipopolysaccharide and p53-inducible gene, LITAF(PIG7), and estrogen-inducible gene, EET-1. *J. Biol. Chem.*, **276**, 23065–23076.
23. Ludes-Meyers, J.H., Kil, H., Bednarek, A.K., Drake, J., Bedford, M.T. and Aldaz, C.M. (2004) WWOX binds the specific proline-rich ligand PPXY: identification of candidate interacting proteins. *Oncogene*, **23**, 5049–5055.
24. Saifi, G.M., Szigeti, K., Wiszniewski, W., Shy, M.E., Krajewski, K., Hausmanowa-Petrusewicz, I., Kochanski, A., Reeser, S., Mancias, P., Butler, I. *et al.* (2005) SIMPLE mutations in Charcot-Marie-Tooth disease and the potential role of its protein product in protein degradation. *Hum. Mut.*, **25**, 372–383.
25. Robinson, F.L. and Dixon, J.E. (2005) The phosphoinositide-3-phosphatase MTMR2 associates with MTMR13, a membrane-associated pseudophosphatase also mutated in type 4B Charcot-Marie-Tooth disease. *J. Biol. Chem.*, **280**, 31699–31707.
26. Berger, P., Berger, I., Schaffitzel, C., Tersar, K., Volkmer, B. and Suter, U. (2006) Multi-level regulation of myotubularin-related protein-2 phosphatase activity by myotubularin-related protein-13/set-binding factor-2. *Hum. Mol. Genet.*, **15**, 569–579.
27. Verhoeven, K., De Jonghe, P., Coen, K., Verpoorten, N., Auer-Grumbach, M., Kwon, J.M., FitzPatrick, D., Schmedding, E., De Vriendt, E., Jacobs, A. *et al.* (2003) Mutations in the small GTP-ase late endosomal protein RAB7 cause Charcot-Marie-Tooth type 2B neuropathy. *Am. J. Hum. Genet.*, **72**, 722–727.
28. Zuchner, S., Noureddine, M., Kennerson, M., Verhoeven, K., Claeys, K., De Jonghe, P., Merory, J., Oliveira, S.A., Speer, M.C., Stenger, J.E. *et al.* (2005) Mutations in the pleckstrin homology domain of dynamin 2 cause dominant intermediate Charcot-Marie-Tooth disease. *Nat. Genet.*, **37**, 289–294.
29. Jager, S., Bucci, C., Tanida, I., Ueno, T., Kominami, E., Saftig, P. and Eskelinen, E.L. (2004) Role for Rab7 in maturation of late autophagic vacuoles. *J. Cell Sci.*, **117**, 4837–4848.
30. Harrison, R.E., Bucci, C., Vieira, O.V., Schroer, T.A. and Grinstein, S. (2003) Phagosomes fuse with late endosomes and/or lysosomes by extension of membrane protrusions along microtubules: role of Rab7 and RILP. *Mol. Cell Biol.*, **23**, 6494–6506.
31. Press, B., Feng, Y., Hoflack, B. and Wandinger-Ness, A. (1998) Mutant Rab7 causes the accumulation of cathepsin D and cation-independent mannose 6-phosphate receptor in an early endocytic compartment. *J. Cell Biol.*, **140**, 1075–1089.
32. Tanabe, K. and Takei, K. (2009) Dynamic instability of microtubules requires dynamin 2 and is impaired in a Charcot-Marie-Tooth mutant. *J. Cell Biol.*, **185**, 939–948.
33. Hinshaw, J.E. (2000) Dynamin and its role in membrane fission. *Annu. Rev. Cell Dev. Biol.*, **16**, 483–519.
34. Schafer, D.A., Weed, S.A., Binns, D., Karginov, A.V., Parsons, J.T. and Cooper, J.A. (2002) Dynamin2 and cortactin regulate actin assembly and filament organization. *Curr. Biol.*, **12**, 1852–1857.
35. Thompson, H.M., Cao, H., Chen, J., Euteneuer, U. and McNiven, M.A. (2004) Dynamin 2 binds gamma-tubulin and participates in centrosome cohesion. *Nat. Cell Biol.*, **6**, 335–342.
36. Boutin, J.A. (1997) Myristoylation. *Cell Signal.*, **9**, 15–35.
37. Maurer-Stroh, S., Eisenhaber, B. and Eisenhaber, F. (2002) N-terminal N-myristoylation of proteins: refinement of the sequence motif and its taxon-specific differences. *J. Mol. Biol.*, **317**, 523–540.
38. Resh, M.D. (1999) Fatty acylation of proteins: new insights into membrane targeting of myristoylated and palmitoylated proteins. *Biochim. Biophys. Acta*, **1451**, 1–16.
39. Martinez-Rubio, D., Millan, J.M., Palau, F. and Espinos, C. (2008) Gene symbol: SH3TC2. Disease: Charcot-Marie-Tooth type 4C. *Hum. Genet.*, **124**, 320.
40. Peitzsch, R.M. and McLaughlin, S. (1993) Binding of acylated peptides and fatty acids to phospholipid vesicles: pertinence to myristoylated proteins. *Biochemistry*, **32**, 10436–10443.
41. Morton, C.J. and Campbell, I.D. (1994) SH3 domains. Molecular 'Velcro'. *Curr. Biol.*, **4**, 615–617.
42. Mayer, B.J. (2001) SH3 domains: complexity in moderation. *J. Cell Sci.*, **114**, 1253–1263.
43. Pawson, T. (1995) Protein modules and signalling networks. *Nature*, **373**, 573–580.
44. Blatch, G.L. and Lassle, M. (1999) The tetratricopeptide repeat: a structural motif mediating protein-protein interactions. *Bioessays*, **21**, 932–939.
45. McPherson, P.S. (1999) Regulatory role of SH3 domain-mediated protein-protein interactions in synaptic vesicle endocytosis. *Cell Signal.*, **11**, 229–238.
46. Kim, Y. and Chang, S. (2006) Ever-expanding network of dynamin-interacting proteins. *Mol. Neurobiol.*, **34**, 129–136.
47. Seaman, M.N. (2008) Endosome protein sorting: motifs and machinery. *Cell Mol. Life Sci.*, **65**, 2842–2858.
48. Ghosh, R.N., Mallet, W.G., Soe, T.T., McGraw, T.E. and Maxfield, F.R. (1998) An endocytosed TGN38 chimeric protein is delivered to the TGN after trafficking through the endocytic recycling compartment in CHO cells. *J. Cell Biol.*, **142**, 923–936.
49. Hunt, K.A., McGovern, D.P., Kumar, P.J., Ghosh, S., Travis, S.P., Walters, J.R., Jewell, D.P., Playford, R.J. and van Heel, D.A. (2005) A common CTLA4 haplotype associated with coeliac disease. *Eur. J. Hum. Genet.*, **13**, 440–444.
50. Niemann, A., Berger, P. and Suter, U. (2006) Pathomechanisms of mutant proteins in Charcot-Marie-Tooth disease. *Neuromolecular Med.*, **8**, 217–242.
51. Wishart, M.J. and Dixon, J.E. (2002) PTEN and myotubularin phosphatases: from 3-phosphoinositide dephosphorylation to disease. *Trends Cell Biol.*, **12**, 579–585.
52. Vonderheit, A. and Helenius, A. (2005) Rab7 associates with early endosomes to mediate sorting and transport of Semliki forest virus to late endosomes. *PLoS Biol.*, **3**, e233.

53. Ryan, M.C., Shooter, E.M. and Notterpek, L. (2002) Aggresome formation in neuropathy models based on peripheral myelin protein 22 mutations. *Neurobiol. Dis.*, **10**, 109–118.
54. von Zastrow, M. and Sorkin, A. (2007) Signaling on the endocytic pathway. *Curr. Opin. Cell Biol.*, **19**, 436–445.
55. Altschul, S.F., Gish, W., Miller, W., Myers, E.W. and Lipman, D.J. (1990) Basic local alignment search tool. *J. Mol. Biol.*, **215**, 403–410.
56. Coppi, M.V. and Guidotti, G. (1997) Intracellular localization of Na,K-ATPase alpha2 subunit mutants. *Arch. Biochem. Biophys.*, **346**, 312–321.